ELSEVIER

Experimental Hematology

Experimental Hematology 2018;■■:■■–■■

Loss of DEK induces radioresistance of murine restricted hematopoietic progenitors

Juana Serrano-Lopez[a,b], Kalpana Nattamai[a,b], Nicholas A. Pease[a,b,1], Miranda S. Shephard[a,b], Ashley M. Wellendorf[a,b], Mathieu Sertorio[a,b], Eric A. Smith[a,b], Hartmut Geiger[a,b], Susanne I. Wells[a,b], Jose A. Cancelas[a,b], and Lisa M. Privette Vinnedge[a,b]

[a]*Cancer and Blood Diseases Institute, Cincinnati Children's Hospital Medical Center, Cincinnati, Ohio;* [b]*Department of Pediatrics, University of Cincinnati College of Medicine, Cincinnati, Ohio*

(Received 28 July 2017; revised 15 December 2017; accepted 19 December 2017)

Self-renewing hematopoietic stem cells and multipotent progenitor cells are responsible for maintaining hematopoiesis throughout an individual's lifetime. For overall health and survival, it is critical that the genome stability of these cells is maintained and that the cell population is not exhausted. Previous reports have indicated that the DEK protein, a chromatin structural protein that functions in numerous nuclear processes, is required for DNA damage repair in vitro and long-term engraftment of hematopoietic stem cells in vivo. Therefore, we investigated the role of DEK in normal hematopoiesis and response to DNA damaging agents in vivo. Here, we report that hematopoiesis is largely unperturbed in DEK knockout mice compared with wild-type (WT) controls. However, DEK knockout mice have fewer radioprotective units, but increased capacity to survive repeated sublethal doses of radiation exposure compared with WT mice. Furthermore, this increased survival correlated with a sustained quiescent state in which DEK knockout restricted hematopoietic progenitor cells (HPC-1) were nearly three times more likely to be quiescent following irradiation compared with WT cells and were significantly more radioresistant during the early phases of myeloid reconstitution. Together, our studies indicate that DEK functions in the normal hematopoietic stress response to recurrent radiation exposure.

Hematopoietic stem cells (HSCs) and multipotent progenitor (MPP) cell populations are lifelong cell populations that are needed to maintain blood production. HSCs give rise to long-lived MPP cells with limited self-renewal capacity, which then produce the more differentiated progenitor cells responsible for steady-state blood production. Bone marrow injury is a loss of self-renewing HSC reserves that can be a result of prolonged or repeated exposure to toxic agents, such as chemotherapy or radiotherapy for cancer [1,2]. Recurrent or severe bone marrow injury can result in the loss of these primitive hematopoietic cells and, eventually, mortality caused by exhaustion of the HSC and MPP populations and the subsequent inability to produce mature blood cells. Therefore, HSC survival and maintenance of proper hematopoiesis constitute an important limit on treatment dose during cancer therapy. Long-term bone marrow injury often coincides with mutations introduced by the hematopoietic stress agents and is a risk factor for leukemia and myelodysplastic syndromes (MDSs). In fact, nearly 30% of cases of MDS are attributed to bone marrow injury after chemotherapy or radiotherapy [3].

One mechanism through which long-lived hematopoietic stem and progenitor cells (HSC/Ps) protect their genome is by entering a state of cellular quiescence, which protects the cells from reactive oxygen species and replication-mediated DNA damage [4]. As with other cell types, quiescent HSCs depend on nonhomologous end joining (NHEJ) for DNA damage repair—a mechanism that does not require a sister chromatid template and is relatively error prone [4,5]. This is thought to be one source of mutations in HSCs that

Offprint requests to: Lisa M. Privette Vinnedge, PhD, Cincinnati Children's Hospital Medical Center, Division of Oncology, MLC 7013, 3333 Burnet Avenue, Cincinnati, OH 45229; E-mail: Lisa.Privette@cchmc.org

[1]Present address: Department of Bioengineering, University of Washington, Seattle, WA 98195.

Supplementary data related to this article can be found online at https://doi.org/10.1016/j.exphem.2017.12.009.

https://doi.org/10.1016/j.exphem.2017.12.009

accumulate over an organism's lifetime and contribute to the overall aging of the hematopoietic system. In response to hematopoietic stress, such as radiation exposure, quiescent HSCs are activated and begin proliferating to replenish the hematopoietic system. Proliferating HSCs, as well as other proliferating populations like progenitor cells, depend on homologous recombination (HR) for DNA damage repair. HR requires the presence of a sister chromatid for repair and is thought to be relatively error free, thus minimizing the accumulation of mutations. In accordance with the importance of DNA damage repair in HSCs and MPP cells, many inherited disorders in DNA repair pathways (i.e., ataxia telangiectasia and Fanconi anemia) include a very high incidence of bone marrow failure and MDS. Thus, genome stability, DNA repair, and other cellular responses to chronic hematological stress are critical factors in the long-term survival of healthy HSC and MPP cells and in limiting the risk for hematological disease.

In the adult mouse, all multipotent cells are contained in the Lineage$^{-/low}$Sca-1^{+}c-Kit^{+} (LSK) fraction of bone marrow cells, though this population is very heterogeneous [6–8]. Lineage$^{-/low}$Sca-1^{+}c-kit^{+} (LSK) cells can be subdivided into four fractions based on the expression of CD150 and CD48: HSCs are CD150^{+}CD48^{-}LSK, MPP cells are CD150^{-}CD48^{-}LSK, and CD150^{-}CD48^{+}LSK (hematopoietic progenitor cell [HPC]-1) and CD150^{+}CD48^{+}LSK (HPC-2) cells contain heterogeneous restricted progenitors [9–11]. Despite markers that can give high levels of HSC and MPP purity, HSC and MPP populations remain functionally heterogeneous. Competitive repopulation experiments, in which repopulating test HSC/Ps mixed with competitor wild-type (WT) bone marrow cells are infused into a recipient, can identify the commitment of the HSCs and progenitors in irradiated recipient mice. Although HSCs are responsible for long-term repopulation of the entire hematopoietic system, progenitors are capable only of short-term repopulation of more or less restricted hematopoietic cell lineages. The relative fitness of genetically modified HSC/Ps can be directly compared through a competitive repopulation assay, in which isolated HSC from two genetically distinct donors are mixed prior to transplantation into lethally irradiated mice [12].

Previously, the DEK protein was found to be necessary for long-term engraftment of hematopoietic stem cells [13]. DEK is a structural protein of chromatin with histone H3.3 chaperone activity [14,15]. Its activity has been implicated in regulating several nuclear processes, including DNA replication, transcription, and DNA repair by both NHEJ and HR [16–19]. DEK is most frequently described as an oncogene in most solid tumors and as a fusion partner with CAN/NUP214 in MDS and t(6;9) acute myeloid leukemia (AML), which correlates with a poor survival rate [20]. However, decreased DEK expression, compared with normal human bone marrow, has been observed in cases of AML that do not have the t(6;9) translocation [21]. In normal hematopoietic cells, DEK suppresses the proliferation of early myeloid progenitors [13]. This is evidenced both in the increased number of colony-forming units–granulocyte/macrophage (CFU-GM) produced by bone marrow cells from DEK knockout (KO) mice compared with WT mice and in the reduction of these colonies when recombinant DEK was added to the cultures of either murine bone marrow cells or CD34^{+} human cord blood [13]. Furthermore, DEK promoted granulocytic differentiation in CD34^{+} human bone marrow cells treated with granulocyte colony-stimulating factor (G-CSF) [22]. In that study of myeloid differentiation, DEK depletion by shRNA in CD34^{+} cells reduced the number of granulocytic colonies (CFU-G), but increased the number of bipotent CFU-GM. This promotion of myeloid differentiation was due, in part, to DEK binding to dephosphorylated C/EBPα to stimulate the transcription of myeloid differentiation genes, such as *GCSFR3* [22]. Collectively, the data indicate that DEK negatively regulates the proliferation of early myeloid progenitors and promotes the differentiation of mature myeloid cells.

We investigated in more detail the role of DEK in hematopoiesis, with a focus on HSC/Ps. In addition, given its role in stress responses and DNA damage repair following irradiation in vitro, we also investigated the role of DEK in the cellular and organismal response to radiation-induced DNA damage in vivo using previously reported WT and DEK KO mice [23]. Here, we illustrate that murine DEK is necessary for proper hematopoietic MPP cell responses to radiation-induced damage, likely via regulation of the cellular decision to maintain quiescence versus enter a proliferative state.

Methods

Mice

DEK$^{-/-}$ mice were originally kindly donated by Gerard Grosveld (St. Jude Children's Research Hospital, Memphis, TN) and have been previously described [23]. The mice were generated and maintained on a mixed C57BL/6/129/SVEV background. *DEK*$^{+/+}$ and *DEK*$^{-/-}$ were obtained by mating heterozygous parents. C57BL/6 (CD45.2^{+}/Ly5.2) mice between 8 and 10 weeks of age were purchased from both Jackson Laboratory (Bar Harbor, ME) and Harlan Laboratories (Frederick, MD). B6.SJL$^{Ptprca\ Pepcb/BoyJ}$ (CD45.1^{+}/Ly5.1) mice were obtained from the Division of Experimental Hematology/Cancer Biology of the Cincinnati Children's Hospital Research Foundation (CCHRF). Handling of mice was performed with the approval of the Cincinnati Children's Institutional Animal Care and Use Committee. All mice were housed in specific pathogen-free housing with ad libitum access to food and water.

Quantitative real-time polymerase chain reaction

RNA isolation from the samples isolated from C57Bl/6 animals was performed with the RNeasy Micro Kit from Qiagen (Germantown, MD, USA). The level of RNA expression was determined by real-time reverse transcription polymerase chain reaction (RT-PCR) using Taqman Universal PCR and RT reagents from Applied Biosystems (ThermoFisher, Carlsbad CA, USA). Expression was quantified with the standard curve method. All real-time PCRs were run with TaqMan real-time PCR reagent and primers from Applied Biosystems on an ABI9700HT real-time machine.

Colony-forming cell assay

Colony-forming cell (CFC) assays were performed using Methocult (M3234 Stem Cell Technologies, Vancouver, BC, Canada). Total bone marrow (BM) cells (2×10^5) were plated in triplicate in six-well plates. Plates were incubated at 37°C in 5% CO_2, and colonies were counted between 7 and 10 days after plating.

Immunostaining and cell sorting for transplantation studies

For early hematopoiesis analysis, mononuclear cells were isolated by low-density centrifugation (Histopaque 1083, Sigma Aldrich) and stained with a cocktail of biotinylated lineage antibodies. Biotinylated antibodies used for lineage staining were all rat anti-mouse antibodies: anti-CD11b (clone M1/70), anti-B220 (clone RA3-6B2), anti-CD3 (clone 53-7.3), anti-Gr-1 (clone RB6-8C5), anti-Ter119, and anti-CD8a (clone 53-6.7) (all from eBioscience/ThermoFisher, Carlsbad, CA). After lineage depletion by magnetic separation (Dynalbeads, Invitrogen/ThermoFisher, Carlsbad, CA), cells were stained with anti-Sca-1 (clone D7), anti-c-Kit (clone 2B8), anti-CD34 (clone RAM34), anti-Flk-2 (clone A2F10), and streptavidin (all from eBioscience). Early hematopoiesis fluorescence-activated cell sorting (FACS) analysis data were plotted as percentages of long-term HSCs (LT-HSCs; gated as LSK $CD34^{-/low}Flk2^-$), short-term HSCs (ST-HSCs; gated as LSK $CD34^+Flk2^-$), lymphoid-primed MPPs (LMPPs; gated as LSK $CD34^+Flk2^+$), and distributed LSKs ($Lin^{neg}c\text{-}Kit^+Sca\text{-}1^+$ cells). To isolate all the cell types, lineage depletion was performed to enrich for lineage-negative cells. Lineage-negative cells were then stained as described above and sorted using a BD FACS Aria III (BD Biosciences, San Jose, CA, USA).

Immunostaining and flow cytometry analyses were performed according to standard procedures using a FACSCanto flow cytometer (BD Biosciences). Anti-Ly5.2 (clone 104, BD Biosciences, fluorescein isothiocyanate [FITC] conjugated) and anti-Ly5.1 (clone A20, BD Biosciences, phycoerythrin [PE] conjugated) monoclonal antibodies were used to distinguish donor from recipient and competitor cells. For lineage analysis in hematopoietic tissues, anti-CD3ε (clone 145-2C11), anti-B220 (clone RA3-6B2,), anti-CD11b (clone M1/70), and anti-Gr-1 (clone RB6-8C5) were used. Lineage FACS analysis data are plotted as percentages of $B220^+$, $CD3^+$, and myeloid ($Gr\text{-}1^+$, $Mac\text{-}1^+$, and $Gr\text{-}1^+Mac\text{-}1^+$) cells among donor-derived $Ly5.2^+$ cells in transplantation experiments or among total white blood cells (WBCs).

Transplantation assays

For competitive transplantation assays, 1×10^6 total BM cells from either DEK WT mice or DEK KO mice were combined with 1×10^6 total BM cells from a donor Boy J mouse and transplanted into lethally irradiated Boy J mice via tail vein injection. The engraftment potential of the donor cells was followed every 3 weeks for 12 weeks by analysis of peripheral blood (PB) chimerism. For the second competitive transplantation assay, a total of 3×10^5 Boy J BM cells and 10 million donor cells from sublethally irradiated DEK WT or KO mice were combined and transplanted into lethally irradiated BoyJ mice. The engraftment potential of irradiated donor cells was followed every week. To determine the differences in BM microenvironment, 5×10^5 total BM cells from Boy J mice were transplanted via tail vein into either DEK WT or DEK KO mice. The engraftment potential of the BoyJ cells was quantified every 3 weeks for 12 weeks by analysis of PB chimerism.

5-Fluorouracil treatment

DEK WT and KO mice were challenged once with 5-fluorouracil 150 mg/kg body weight. Peripheral blood was collected from the mice before treatment and at different time points after treatment, to analyze the recovery of different lineages by flow cytometry and by cell count using Hemavet (Drew Scientific, Miami Lakes, FL).

Flow cytometry analysis and sorting for HSC/Ps or MPP cells

Erythrocyte-depleted BM cells were stained first for lineage markers with a biotin-labeled mouse lineage panel (BD Biosciences, Pharmingen) containing anti-CD3e ($CD3_\varepsilon$ chain), anti-TER-119/erythroid cells (Ly-76), anti-Gr1 (Ly6G and Ly-6C), anti-CD45R (B220), anti-CD11b (integrin α chain, Mac1α) followed by labeling with allophycocyanin and cyanine dye Cy7-(APC-Cy7)-conjugated streptavidin, PerCP and cyanine dye Cy5.5 (PerCP-Cy5.5)-conjugated anti-c-Kit (clone 2B8), *R*-phycoerythrin and cyanine dye Cy7 (PECy7)-conjugated anti-Sca1 (clone D7), allophycocyanin (APC)-conjugated anti-CD150 (clone 9D1), and FITC-conjugated anti-CD48 (clone HM48-1) (Affymetrix eBioscience, San Diego CA). FACS sequential discrimination on a lineage-negative gated population was used to identify LK myeloid progenitors ($Lin^-c\text{-}Kit^+Sca1^-$). LSK ($Lin^-Sca1^+c\text{-}Kit^-$) subpopulations were distinguished as ($Lin^-c\text{-}Kit^+Sca1^+CD48^-CD150^+$) for HSC and ($Lin^-c\text{-}Kit^+Sca1^+CD48^+CD150^{+/-}$) for MPPs. FACS sorting strategies were ($Lin^-c\text{-}Kit^-Sca1^+CD48^-CD150^+$) for HSCs, ($Lin^-c\text{-}Kit^-Sca1^+CD48^{-/lo}CD150^-$) for MPP cells, ($Lin^-c\text{-}Kit^-Sca1^+CD48^+CD150^-$) for HPC-1, ($Lin^-c\text{-}Kit^-Sca1^+CD48^+CD150^+$) for HPC-2, and ($Lin^-c\text{-}Kit^+Sca1^-$) for mature progenitor LK cells in a FACSAria II cell sorter (BD Biosciences).

Limiting dilution transplantation and radiosensitivity assays

To assess noncompetitive transplantation using limiting dilution of BM cells, we used WT or KO DEK mice as donors to lethally irradiated C57BL/6 mice. Bone marrow HSC frequencies were estimated by Poisson statistics as the reciprocal of the number of test cells that yielded a 37% negative response. To evaluate radioprotection units contained in each group of animals ($n = 6$), we irradiated sublethally (7 Gy) WT and KO DEK mice and analyzed survival curves after four doses spatially performed.

PhosphoFlow, apoptosis, and cell cycle analysis

Mice were exposed to one dose of 7-Gy radiation, and bone marrow was harvested 24 hours later. Cell cycle analysis of HSCPs, MPP cells, and the LK compartment was performed using pyronin Y (0.25 μg/mL/10^6 cells; Sigma-Aldrich, St. Louis, MO) and Hoescht33342 (2 μg/mL/10^6 cells; Invitrogen) dyes. For intracellular analysis of the phosphorylated state of p38 protein into HSCPs, surface antigen-labeled cells were fixed with Cytofix buffer (BD Biosciences) for 20 min and then permeabilized using Cytofix/Cytoperm buffer (BD Bioscience) for 20 min. After being washed, cells were stained intracellularly using Alexa Fluor-647 anti-phospho-p38(clone 36/p38 [pT180/pY182], BD Biosciences) and Alexa Fluor-647 anti-phospho-ERK1/2 (clone 20A, BD Biosciences) for 40 min in Perm/Wash Buffer 1 × (BD Biosciences) with 0.5% of mouse serum. All incubations after cell stimulation were done on ice and in the dark. Cell acquisition was performed by flow cytometry (LSRFortessa I, BD Biosciences) equipped with FACSDIVA software (BD, Biosciences) for multiparametric analysis of the data.

For in vitro quantification of apoptotic mouse embryonic fibroblast cells, an Alexa Fluor-647-labeled cleaved caspase 3 antibody

(Cell Signaling 9602, Danvers, MA, USA) was incubated on methanol-permeabilized cells for 1 hour and analyzed on a BD-FACSCanto II instrument, as reported previously [17].

RNA sequencing

Two mice per genotype were exposed to one dose of 7 Gy radiation, and then 24 hours later, MPP/HCP-1/HCP-2 cells were sorted by FACS and pooled. RNA was isolated with the Qiagen RNeasy Mini Kit, and approximately 80–120 ng of RNA was amplified to generate cDNA. The initial amplification step for all samples was performed with the NuGEN Ovation RNA-Seq System v2 (NuGEN, San Carlos CA, USA). The concentrations were measured using the Qubit dsDNA BR assay. cDNA size was determined by using a DNA 1000 Chip. Libraries were then created for both samples. Specifically, the Nextera XT DNA Sample Preparation Kit (Illumina, San Diego, CA, USA), was used to create DNA library templates from the double-stranded cDNA. Concentrations were measured using the Qubit dsDNA HS assay. Then 1 ng of cDNA was suspended in Tagment DNA buffer. Tagmentation (fragmentation and tagging with the adaptors) was performed with the Nextera enzyme (Amplicon Tagment Mix, Illumina) by incubation at 55°C for 10 min. NT buffer was then added to neutralize the samples. Libraries were prepared by PCR with the Nextera PCR Master Mix and 2 Nextera Indexes (N7XX and N5XX) according to the following program: 1 cycle of 72°C for 3 min; 1 cycle of 98°C for 30 sec; 12 cycles of 95°C for 10 sec, 55°C for 30 sec, and 72°C for 1 min; and 1 cycle of 72°C for 5 min. Purified cDNA was captured on an Illumina flow cell for cluster generation. The size of the libraries for each sample was measured using the Agilent HS DNA chip (Agilent Genomics, Santa Clara CA, USA). Libraries were sequenced on the Illumina HiSeq2500 following the manufacturer's protocol, with 75-bp paired-end sequencing and a coverage of 30M reads.

Quantification of mRNA expression levels was based on the TopHat/Cufflinks pipeline of the CCHMC DNA sequencing and Genotyping Core. Reads were aligned to the mouse mm10/GRCm38 reference genome using TopHat. BAM files containing the aligned reads were used to quantify mRNA expression level using Cufflinks with the USCS known gene reference annotation. RNA expression values were normalized by the reads per kilobase per megabase calculation (RPKM).

Statistics

Mouse survival following repeated radiation exposure was analyzed using the log-rank test. A two-tailed *t*-test with the Bonferroni–Dunn correction method was used to assess significance of changes in blood cell counts over time. Otherwise, an unpaired two-tailed Student *t*-test was used to compare all other data sets. Error bars depict standard errors of data collected from at least three animals. Significance was set at $p < 0.05$ ($*p < 0.05$, $**p < 0.01$).

Results

DEK expression in murine HSC/P populations has not yet been fully characterized. We performed quantitative RT-PCR to determine the relative expression of DEK in the heterogeneous group of HSC/P. DEK expression was highest in the population of differentiated hematopoietic cells (Lin^+ cells). DEK expression was detectable, but lower in HPCs (Lin-c-Kit^+ [LK] cells) and similar across three populations of very primitive hematopoietic cells: LT- and ST-HSCs and MPP cells (Fig. 1A). This agrees with reports of HSCs being largely quiescent: DEK is an E2F target gene and is expressed predominantly in proliferating cells, including activated hematopoietic cells, such as lymphoblasts, and nonquiescent stem cells [24–26].

To determine if DEK is required for HSC/P maintenance, we analyzed the number of cells from the bone marrow of WT ($DEK^{+/+}$) and DEK KO ($DEK^{-/-}$) mice. DEK loss did not, in general, affect the relative numbers of these types of cells in the bone marrow, except for an approximate 35% decrease of LK cells (Fig. 1B). To further examine the role of DEK in HPC biology, we performed colony assays to assess frequency and differentiation of various progenitor populations. Cells isolated from DEK KO mice displayed an increase in the frequency of overall CFU, in line with published data, although this was not accompanied by differences in CFU-Mix, BFU-E (burst forming units–erythroid) or CFU-GM) (Fig. 1C) [13]. Interestingly, we observed a decrease in the number of nucleated cells in the bone marrow of DEK KO mice compared with WT mice, which was mostly accounted for by a significant decrease in B cells (Fig. 1D). However, this decrease in B cells was not apparent in the peripheral blood and was not associated with differences in immunoglobulin class switch recombination (data not shown and [17]).

To investigate whether DEK loss had cell intrinsic effects or affected the bone marrow microenvironment, we performed a series of bone marrow transplantation assays. There was no difference in transplantation efficiency or cell distribution in peripheral blood when CD45.1 BoyJ cells were transplanted into lethally irradiated DEK WT and KO mice over the course of 6 months (Supplementary Figure E1A, online only, available at www.exphem.org and data not shown), indicating that the bone marrow microenvironment is unaffected by DEK loss. To test for cell intrinsic effects of DEK loss and HSC function, we performed competitive transplantation assays, in which bone marrow cells from DEK WT or KO mice were combined with equal numbers of bone marrow cells from BoyJ mice and transplanted into lethally irradiated BoyJ mice. Consistent with previous reports, at 3 weeks (Supplementary Figure E1B, online only, available at www.exphem.org) and up to 12 weeks (data not shown), we detected no differences in primary transplantation efficiency between DEK WT and KO bone marrow cells [13].

Recent in vitro studies identified DEK as a necessary factor for radiation-induced DNA damage repair by homologous recombination [17]. We thus subjected WT ($n = 6$) and KO ($n = 6$) mice to repeated doses of 7-Gy sublethal irradiation (Fig. 2A). Serial sublethal irradiation is an effective approach to identify the effect of DNA damage on the more quiescent primitive progenitor compartment, thus differentiating this from the effects of single doses of radiation on more differentiated, lineage-committed progenitors [27,28]. Surprisingly, DEK KO mice exhibited prolonged survival following serial radiation exposure (Fig. 2B). Increased survival of serially irradiated DEK KO mice was associated with

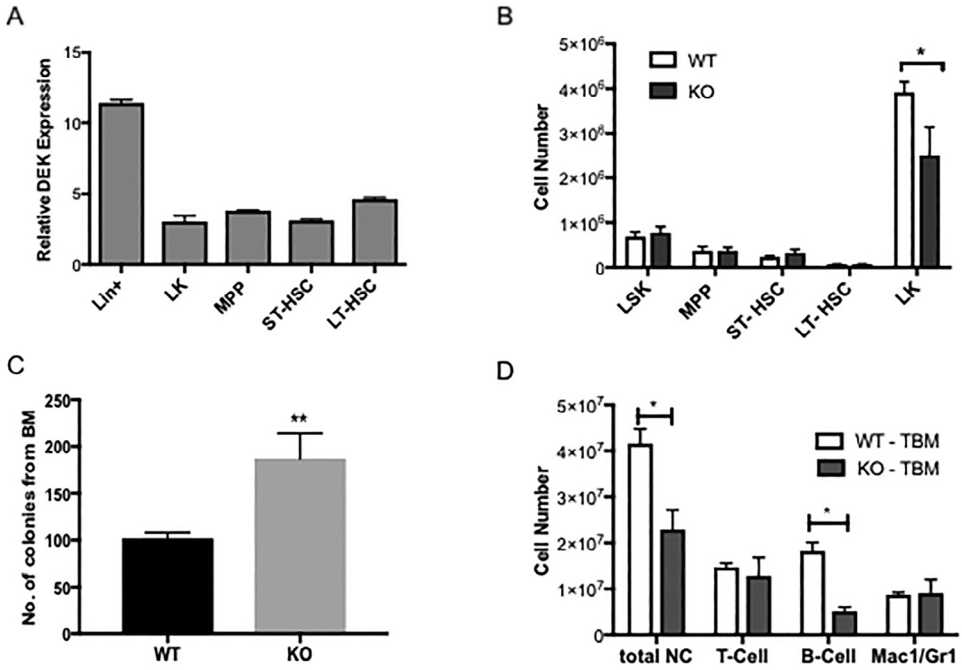

Figure 1. Characterization of DEK expression and impact of DEK loss on differentiation in hematopoietic cell populations. **(A)** Quantitative RT-PCR for DEK expression, relative to β-Actin, reveals that DEK expression is highest in Lin^+ cells, but is also present in Lin^- populations ($n = 3$ mice). **(B)** Flow cytometric analysis of whole bone marrow from $DEK^{+/+}$ (DEK WT) and $DEK^{-/-}$ (DEK KO) mice reveals that relative amounts of LK progenitors are decreased in DEK-deficient mice, whereas less differentiated HSC/Ps are unaffected. **(C)** Bone marrow from DEK KO mice formed more colonies in culture than bone marrow from DEK WT mice. **(D)** Lineage analysis by flow cytometry indicates that bone marrow from DEK KO mice have fewer B cells, resulting in decreased cellularity of nucleated cells. For B–D, $n = 6$ for DEK WT mice and $n = 5$ for DEK KO mice. LT = long-term; ST = short term; TBM = total bone marrow.

resistance to radiation in the peripheral blood. As expected, the total WBC count and platelet count decreased in WT mice after three serial sublethal irradiations; however, the average WBC count increased in KO mice (data not shown). Further analyses revealed that the platelet count was maintained, and the neutrophil count significantly increased over time in DEK KO mice (Supplementary Figure E2A and B, online only, available at www.exphem.org). To determine if differences in radiation response were due to cell intrinsic or microenvironment effects, we transplanted WT $CD5.1^+$ bone marrow cells from BoyJ mice into DEK WT and KO mice. There was no significant difference in survival following a single dose of sublethal irradiation between the two groups, suggesting that the expression of DEK in the nontransplantable, bone marrow microenvironment has little impact on the difference in radiation response (Supplementary Figure E1C, online only, available at www.exphem.org), and its role seems to depend on a direct effect on hematopoietic cells.

To further characterize the role of DEK in the radioprotective hematopoietic progenitor compartment, we performed a limiting dilution analysis in vivo by transplanting different doses of bone marrow cells into lethally irradiated mice.

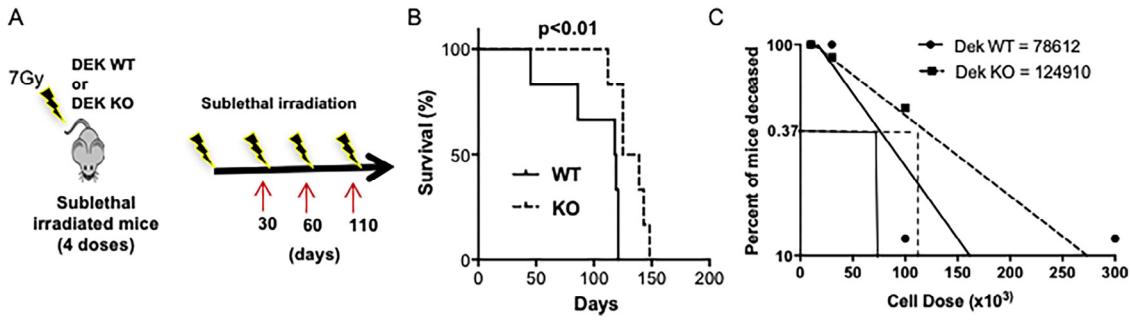

Figure 2. DEK expression is required for proper response to repeated radiation exposure. **(A)** Diagram of experimental methods, in which six mice from each genotype received four sublethal 7-Gy doses of radiation over the course of 110 days. **(B)** Survival curves comparing DEK KO versus WT mice following multiple doses of radiation ($p < 0.01$). **(C)** Bone marrow from DEK WT and KO mice was collected and transplanted into lethally irradiated CD45.2 CD57Bl/6 mice at four doses: 10×10^3, 30×10^3, 100×10^3, and 300×10^3 cells ($n = 8$ mice/group, total of 8 groups).

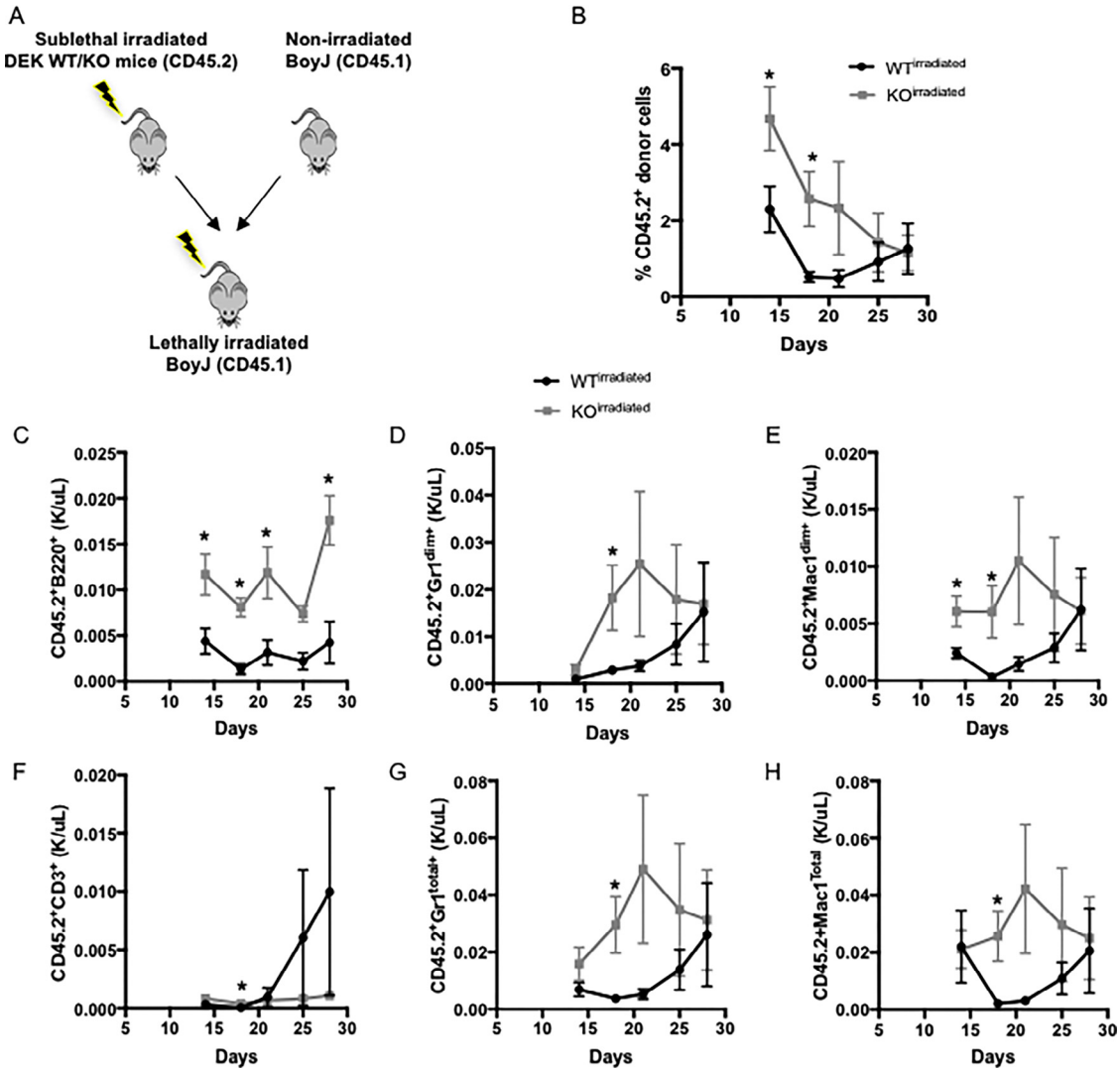

Figure 3. DEK loss induces radioresistance in transient repopulating progenitor cells. **(A)** Diagram of experimental methods in which bone marrow cells were collected from irradiated WT ($n = 5$) or KO ($n = 4$) donor mice and co-transplanted with competitor bone marrow cells from BoyJ mice prior to implantation into lethally radiated BoyJ mice. **(B)** Analysis of peripheral blood chimerism over 28 days, revealing percentage of total CD45.2 nucleated cells from WT versus KO donor mice, as well as $B220^+$ B cells **(C)**, $CD3^+$ T cells **(F)**, and both $Gr1^+$ and $Mac1^+$ myeloid cells **(D, E, G, H).** Irradiated DEK KO cells exhibited better recovery and less stress after transplantation.

The transplantable cells that facilitate the recovery of bone marrow tissue from radiation damage are called radioprotective units. Contrary to their prolonged survival following repeated radiation, bone marrow cells from DEK KO mice contained fewer radioprotective units on transplantation, at 1 in 124,910 cells compared with 1 in 78,612 cells from WT bone marrow (Fig. 2C). This suggests, paradoxically, that DEK loss stimulates radioresistance transferred by transplantable progenitors.

To test this hypothesis, we performed a competitive repopulation assay, in which we combined irradiated DEK WT ($n = 5$) or KO ($n = 4$) bone marrow cells with bone marrow cells from BoyJ competitors prior to transplantation into lethally irradiated BoyJ mice (Fig. 3A). Peripheral blood chimerism was monitored for the next 28 days. Irradiated KO bone marrow cells exhibited improved short-term repopulation during weeks 2–4 immediately post-transplantation compared with WT cells (Fig. 3B), indicating that, indeed, the loss of DEK causes transplantable progenitor cells to be more resistant to radiation. Further analyses revealed that this radioresistance was most notable in both mature B cells (Fig. 3C) and myeloid-committed progenitors, as indicated by the $Gr1^+$ and $Mac1^+$ populations (Fig. 3D, E, G, H). We next wanted to determine if this effect was limited to radiation or was also evident in other types of DNA damage. Unlike radiation, which causes direct DNA double-strand breaks, 5-fluorouracil causes stalled replication forks that eventually cause DNA breaks. Therefore, 5-fluorouracil

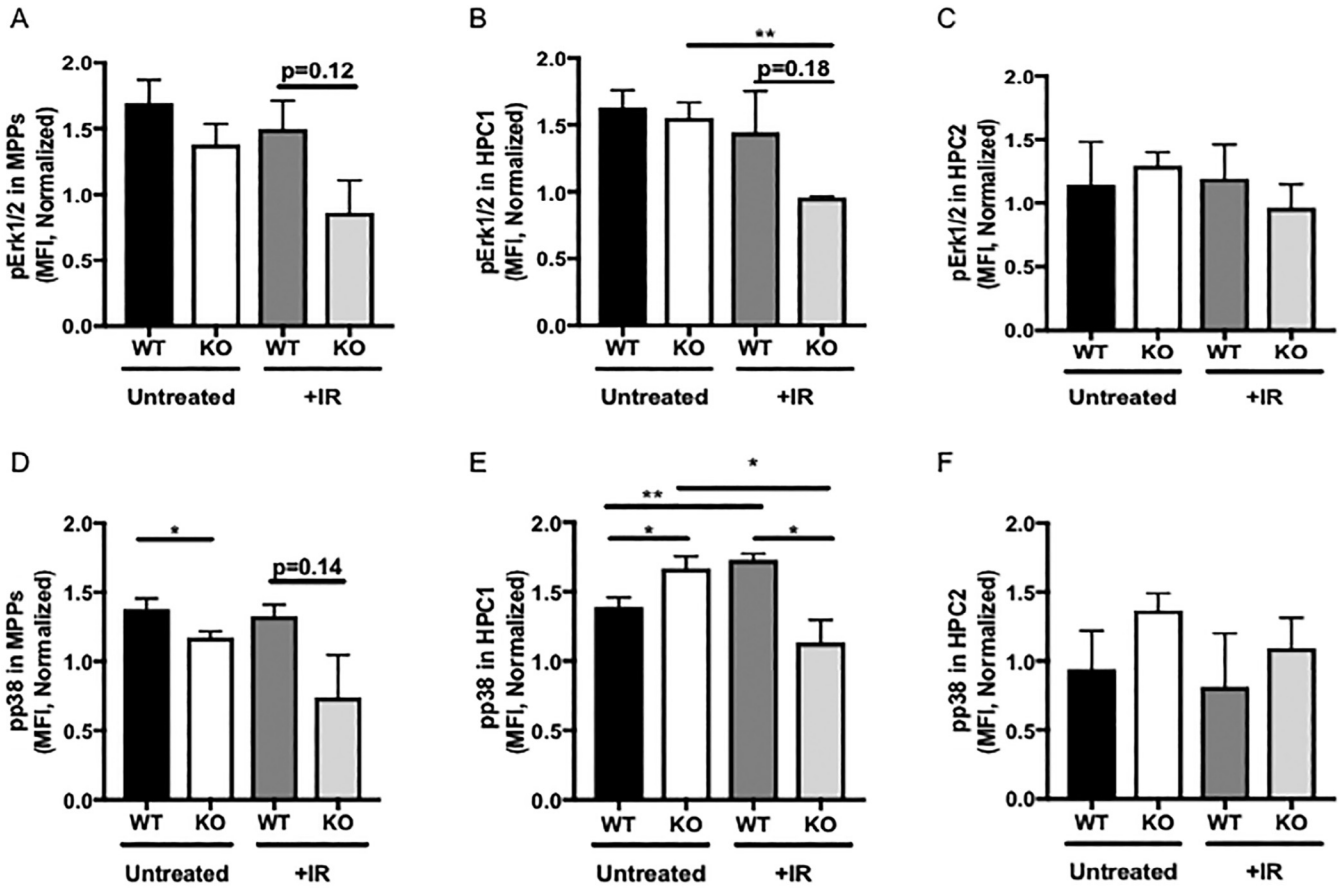

Figure 4. DEK KO progenitor cells exhibit decreased Erk1/2 and p38 phosphorylation in response to irradiation. **(A–C)** Levels of phosphorylated Erk1/2 were modestly downregulated in irradiated DEK KO (A) MPP and (B) HPC-1 cells, but not (C) HPC-2 cells, compared with DEK WT cells. **(D–F)** Levels of phosphorylated p38. (D) In MPP cells, levels of phosphorylated p38 were significantly decreased in MPP cells from DEK KO mice compared with those from WT mice. (E) In the HPC-1 subpopulation, untreated DEK KO cells upregulated phosphorylation of p38, which was aberrantly downregulated following irradiation. (F) Phosphorylated p38 levels in HPC-2 cells did not differ between DEK WT and KO cells in either condition. The graphs depict mean fluorescence intensity (MFI) as determined by flow cytometry. $n = 4$ for each group of untreated animals, and $n = 3$ for each group of irradiated animals.

specifically targets cycling progenitor populations. Although there were no differences in long-term survival or hematopoiesis between DEK WT ($n = 6$) and KO ($n = 5$) animals in response to a single dose of 5-fluorouracil, there was a potential difference in short-term response. At 40 days posttreatment, only 67% of WT mice survived, whereas 100% of KO animals were still alive ($p = 0.17$; Supplementary Figure E3, online only, available at www.exphem.org), but this difference disappeared by day 76. Thus, DEK loss may provide at least a short-term survival advantage for progenitor cells when exposed to DNA damage.

Next, we sought to determine how DEK KO mice could survive repeated doses of radiation despite having fewer radioprotective cells, focusing primarily on the primitive progenitor populations, namely HSC/Ps and MPP cells, which are most likely targeted by repeated radiation exposure. The various mitogen-activated protein kinase (MAPK) pathways have often been implicated in regulating response to ionizing radiation. ERK1/2 signaling is mitogenic, whereas p38 is a stress-associated kinase (reviewed in Dent et al [29].). We used flow cytometry to measure the phosphorylation status of MAPK proteins Erk1/2 and p38. There was a modest decrease in Erk1/2 phosphorylation in HPC-1 cells (Fig. 4B), but otherwise there were no observable differences in active Erk1/2 levels in untreated or irradiated progenitor cells between WT and KO animals (Fig. 4A–C). We next measured the phosphorylation of p38. Again, modest decreases were noted in the MPP population (Fig. 4D) and HPC-2 cells exhibited no significant changes in pathway activation (Fig. 4F), but p38 signaling was most profoundly altered in the HPC-1 subpopulation (Fig. 4E). Under the no-treatment condition, p38 phosphorylation was upregulated in DEK KO cells, suggesting an elevated baseline level of stress in these cells. On exposure to radiation, DEK WT cells appropriately increased stress-activated p38 signaling, as detected by phosphorylated p38; however, DEK KO HPC-1 significantly downregulated p38 phosphorylation (Fig. 4E). Together, this suggests that loss of p38 stress signaling in irradiated DEK

KO HPC-1 cells may contribute to the survival these animals experience in response to radiation.

As previously mentioned, in response to stress, HSCs exit quiescence and enter the cell cycle to reconstitute lost blood cells. A possible explanation for the enhanced survival of DEK KO mice after repeated radiation exposure is that the stem and progenitor populations remain in quiescence and are not exhausted through repeated proliferation. Furthermore, previous studies have linked activation by phosphorylation of p38 in HSC/Ps with exit from quiescence, especially in response to stress, in addition to other pathways that can regulate the transition between quiescence (G0) and the G1 phase of dividing HSC/Ps, such as p53 and cyclin E1 [30–34]. Given the decreased p38 induction in irradiated DEK KO MPP and HPC-1 cells, cell cycle analysis was performed on untreated and irradiated HSC and subpopulations of progenitor cells, including MPP, HCP-1, and HCP-2 cells from WT and KO mice (Fig. 5A). The percentage of quiescent (G0) cells was quantified by Hoechst33342 and pyronin Y staining by flow cytometry in WT and KO mice either untreated or after one 7-Gy dose of ionizing radiation. In WT and KO animals, there were no significant differences in the percentage of quiescent (G0) cells in the HSC population under no treatment or irradiation (Fig. 5B–E). MPP cells ($Lin^-c\text{-}Kit^+Sca1^+CD48^{-/lo}CD150^-$) from KO animals were more likely to be in a quiescent state in the no-treatment condition and not cycling as determined by the percentage of cells in S phase, compared with WT controls. This difference was not as pronounced after irradiation (Fig. 5F–I). In agreement with the analysis of the phosphorylated MAPK pathways described above, the most significant differences in radiation response between WT and KO cells was observed in the HCP-1 population ($Lin^-c\text{-}Kit^+Sca1^+CD48^+CD150^-$). HCP-1 cells from KO mice were nearly three times more likely to be quiescent after irradiation compared with DEK WT controls, and this quiescence was accompanied by a significant decline in cycling S-phase cells (Fig. 5J–M). However, HCP-2 cells were not significantly affected by radiation exposure (Fig. 5M–Q). Further analysis of these data to quantify sub-G1 DNA content suggested that DEK KO progenitor cells (Supplementary Figure E4A, online only, available at www.exphem.org), as well as mouse embryonic fibroblasts (Supplementary Figure E4B online only, available at www.exphem.org) isolated from these mice, were less likely to undergo apoptosis in response to irradiation. Therefore, we conclude that DEK KO mice survive repeated radiation exposures because of HPCs that maintain quiescence, with a trend toward a concurrent decrease in apoptosis.

Because there was only a trend toward differences in p38 signaling in DEK KO versus WT MPP cells, we sought to elucidate other molecular mechanism(s) for this difference in radiation response. We performed RNA sequencing on progenitor cells (MPP, HCP-1, and HCP-2) isolated from irradiated WT and KO mice. We found that 120 genes were downregulated at least twofold and 391 genes were upregulated in KO cells compared with WT cells. Gene ontology analyses using ToppGene identified response to gamma radiation ($p = 7.92E\text{-}6$) as a pathway downregulated in DEK KO mouse MPP cells. The following gene ontology groups classified genes with increased expression in DEK KO MPP cells: (1) cellular proliferation, $p = 9.55E\text{-}5$; (2) glutathione derivative processes/glutathione transferase activity, $p = 3.49E\text{-}4$; and (3) regulation of myeloid cell differentiation, $p = 5.93E\text{-}3$. Gene set enrichment analysis also revealed that the p53 signaling pathway was generally downregulated in KO MPP cells (Supplementary Figure E5, online only, www.exphem.org). Further analysis identified several genes that regulate the transition from G0 quiescence to G1 phase and cell cycle entry, including decreases in expression of the genes for cyclin E1, cdk2, and c-Fos and increased expression of genes for $p27^{Kip1}$ and Arf, which both inhibit cyclin E/cdk2 activity to maintain quiescence. Notably, the pro-apoptotic genes *Bid, Bad,* and *Diablo* were also decreased twofold in DEK KO MPP cells compared with WT cells (Table 1). Together, our data support the conclusion that MPP cells from DEK KO mice are more likely to remain quiescent following bone marrow injury from repeated radiation exposure, thus resulting in prolonged animal survival.

Discussion

DEK is an E2F target gene and is therefore most highly expressed in proliferating cells, including progenitor cells, whereas expression is significantly downregulated in quiescent or fully differentiated cells [24,35]. Although the function of DEK during cellular proliferation is still poorly understood, DEK has been reported to promote replication fork progression and help prevent strand breakage at stalled forks [19]. Additional studies have implicated DEK in mediating cellular responses to genotoxic stress, including the promotion of both NHEJ and HR [17,18,36,37]. Molecular DEK activities in these processes, particularly HR and DNA replication, likely involve its affinity for binding cruciform DNA structures [38]. Thus, we hypothesized that DEK may play a significant role in DNA damage responses in murine HPCs. DEK KO animals were expected to display diminished survival in response to repeated exposure to radiation. To some degree, this was observed as a decrease in the number of radioprotective units. However, DEK KO animals exhibited prolonged survival following irradiation, in the absence of significant differences in cell cycle distribution or exit from quiescence within the HSC compartment of DEK KO and WT mice. Further analysis indicated that increased survival is likely due to the maintenance of a protective quiescent state for HPCs, in line with repression of cyclin E/cdk2 mRNA levels in DEK KO progenitor cells, instead of the typical proliferation induction. This also correlated with a decrease in the apoptotic response to radiation in DEK KO cells compared with WT cells that was accompanied by decreased expression of the pro-apoptotic genes *Bid, Bad*, and *Diablo*.

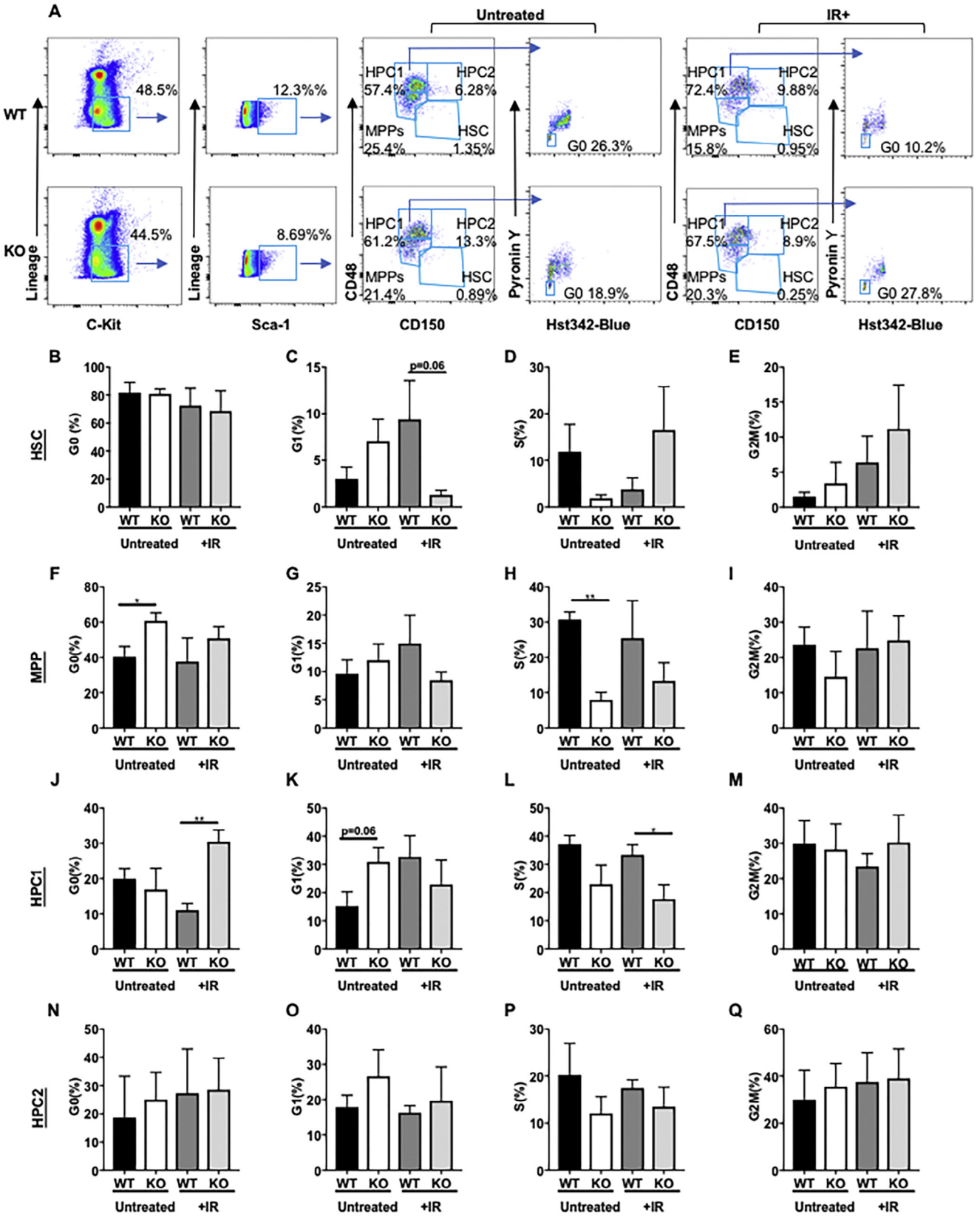

Figure 5. DEK-deficient progenitors become quiescent following irradiation. **(A)** Gating strategy for cell cycle analysis of HSC/P populations in DEK mice after sublethal irradiation. **(B–Q)** Cell cycle analysis of the hematopoietic stem cell and progenitor compartments in untreated ($n = 4$ each genotype) and irradiated ($n = 5$ each genotype) DEK WT and KO mice ($n = 5$). The percentages of cells in G0/quiescence (B, F, J, N), G1 phase (C, G, K, O), S phase (D, H, L, P) and G2M phase (E, I, M, Q) shown were determined after FACS analysis. IR = irradiation.

Table 1. Cell cycle and apoptosis-related genes identified from RNA sequencing of irradiated DEK WT and KO MPP cells

Gene (protein)	Fold change (relative to DEK WT)	Function
Downregulated		
Ccne1 (Cyclin E1)	−2.2855952	Promotes exit from quiescence and induction of cell cycle
Fos (c-Fos; AP-1)	−2.3959737	Induces gene expression of cell cycle-promoting proteins
Bid (BID)	−1.8622921	Pro-apoptotic and triggers cytochrome c release from mitochondria
Diablo (SMAC/Diablo)	−1.8633854	Represses inhibitors of apoptosis, permits caspase activation
Bad (BAD)	−1.8003731	Pro-apoptotic protein that inhibits Bcl-2
Cdk2 (Cdk2)	−1.6217639	Promotes exit from quiescence and G1 and induction of cell cycle
Upregulated		
Cdkn1b ($p27^{Kip1}$)	1.55997328	Inhibits cyclin E/cdk2 activity to promote cell cycle arrest and quiescence
Cdk2ap2 (Arf)	1.50504052	Promotes p53 stabilization and inhibits cyclin E/cdk2 activity

Future studies will investigate if the key role of DEK in this scenario is to regulate proliferation versus quiescence in the hematopoietic system, and whether radiation-induced DNA damage repair pathways are involved. Given the roles of DEK in both DNA replication and repair, it is possible that DEK is necessary for both.

We found that during normal murine hematopoiesis, DEK is most highly expressed in the Lin^+ cell population, for which detailed analyses have already been published [21]. Our data support the concept that the loss of *DEK* most significantly regulates the early HPC populations, including MPPs and LK cells. Specifically, our work indicates that DEK normally facilitates cellular activation and exit from quiescence (G0) in response to radiation exposure. However, under these same experimental conditions, DEK suppresses proliferation and differentiation in late progenitors (i.e., granulocyte–monocyte progenitors), as indicated by the maintenance of neutrophil and platelet counts in KO versus WT mice. This is further supported by previous findings that DEK inhibited the proliferation of more committed progenitor cell populations [13]. Therefore, further research is needed to determine the significance of seemingly opposing DEK activities in early versus late hematopoietic progenitors and their impact on self-renewal versus differentiation.

Furthermore, under steady-state conditions we documented persistent, aberrant p38 activation in untreated DEK KO HPC-1 cells compared with WT cells. Aberrant hyperactivation of p38 signaling is also documented in progenitor cells from patients and murine models with MDS and Fanconi anemia and is associated with decreased progenitor and HSC self-renewal and rapid differentiation. Treatment of hematopoietic progenitors with p38 inhibitors improves progenitor function and promotes self-renewal instead of differentiation [39,40]. However, unlike WT cells, DEK KO HPC-1 cells did not further activate p38 signaling in response to irradiation, which was associated with a threefold increase in quiescence, as well as decreases in proliferation and apoptosis. This agrees with previous work that indicated p38 activation is needed to induce HSC/P proliferation during stress hematopoiesis [34]. Additional work is needed to determine the molecular mechanism by which DEK influences p38 phosphorylation.

Importantly, in three independent assays involving cellular stress, DEK KO cells exhibited increased survival even though there were fewer cells. First, forced cellular proliferation of progenitor cells using in vitro colony-forming assays revealed that cells from DEK KO bone marrow formed more colonies despite having fewer LK progenitor cells. Second, DEK KO mice exhibited increased survival with repeated radiation exposure despite having fewer radioprotective units in the bone marrow. Third, DEK KO mice exposed increased short-term survival following a single dose of 5-FU. Molecular and RNA sequencing analyses suggest this may be due to a combination of decreased apoptosis under stress conditions, perhaps associated with aberrant p38 pathway activation, and differences in cell cycle kinetics and quiescence. Interestingly, this scenario agrees with a study of DEK in *Arabidopsis thaliana,* wherein *DEK* knockout plants exhibited increased germination and survival under stressful high-salt and high-heat conditions, but no obvious health impairments under normal conditions [41]. Overall, we posit that DEK is important for cellular/organismal stress responses to harsh environmental conditions. The loss of DEK may prolong organism survival, at least temporarily, under extreme environmental stress. This, however, may come at the expense of genome integrity, long-term organismal health, and ultimately species preservation. Finally, given that DEK loss promotes progenitor cell survival in the context of radiation, particularly myeloid progenitors, and impairs myeloid differentiation, future studies must now determine whether DEK loss may confer a risk for myeloid leukemia.

Acknowledgments

This work was supported by National Institutes of Health Grants R01-GM110628 (JAC), R01-CA116316 (SIW), and K12HD051953 (LMPV). We acknowledge the contributions of the Research Flow Cytometry Facility and Mouse Core, supported by the NIDDK Center for Excellence in Molecular Hematology (P30-DK090971). JSL was supported by the Government of the Spanish Junta de Andalucia. Work in the laboratory of HG was supported by the Edward P. Evans Foundation and the National Institute of Health (AG040118, DK104814, and AG050650) and the Deutsche Forschungsgemeinschaft (SFB 1074 and SFB1149). We also

thank Marie Matrka for critical reading of the manuscript and Adam Lane for advice regarding statistical analyses.

References

1. Wang Y, Probin V, Zhou D. Cancer therapy-induced residual bone marrow injury: mechanisms of induction and implication for therapy. Curr Cancer Ther Rev. 2006;2:271–279.
2. Biechonski S, Yassin M, Milyavsky M. DNA-damage response in hematopoietic stem cells: an evolutionary trade-off between blood regeneration and leukemia suppression. Carcinogenesis. 2017;38:367–377.
3. Vardiman JW, Thiele J, Arber DA, et al. The 2008 revision of the World Health Organization (WHO) classification of myeloid neoplasms and acute leukemia: rationale and important changes. Blood. 2009;114:937–951.
4. Wilson A, Laurenti E, Oser G, et al. Hematopoietic stem cells reversibly switch from dormancy to self-renewal during homeostasis and repair. Cell. 2008;135:1118–1129.
5. Bakker ST, Passegue E. Resilient and resourceful: genome maintenance strategies in hematopoietic stem cells. Exp Hematol. 2013;41:915–923.
6. Spangrude GJ, Heimfeld S, Weissman IL. Purification and characterization of mouse hematopoietic stem cells. Science. 1988;241:58–62.
7. Ikuta K, Weissman IL. Evidence that hematopoietic stem cells express mouse c-kit but do not depend on steel factor for their generation. Proc Natl Acad Sci USA. 1992;89:1502–1506.
8. Uchida N, Aguila HL, Fleming WH, Jerabek L, Weissman IL. Rapid and sustained hematopoietic recovery in lethally irradiated mice transplanted with purified Thy-1.1^{lo}Lin^{-}Sca^{-}1^{+} hematopoietic stem cells. Blood. 1994;83:3758–3779.
9. Kiel MJ, Yilmaz OH, Iwashita T, Yilmaz OH, Terhorst C, Morrison SJ. SLAM family receptors distinguish hematopoietic stem and progenitor cells and reveal endothelial niches for stem cells. Cell. 2005;121:1109–1121.
10. Kiel MJ, Yilmaz OH, Morrison SJ. CD150^{-} cells are transiently reconstituting multipotent progenitors with little or no stem cell activity. Blood. 2008;111:4413–4414. author reply 4414–4415.
11. Oguro H, Ding L, Morrison SJ. SLAM family markers resolve functionally distinct subpopulations of hematopoietic stem cells and multipotent progenitors. Cell Stem Cell. 2013;13:102–116.
12. Harrison DE. Competitive repopulation: a new assay for long-term stem cell functional capacity. Blood. 1980;55:77–81.
13. Broxmeyer HE, Kappes F, Mor-Vaknin N, et al. DEK regulates hematopoietic stem engraftment and progenitor cell proliferation. Stem Cells Dev. 2012;21:1449–1454.
14. Ivanauskiene K, Delbarre E, McGhie JD, Kuntziger T, Wong LH, Collas P. The PML-associated protein DEK regulates the balance of H3.3 loading on chromatin and is important for telomere integrity. Genome Res. 2014;24:1584–1594.
15. Sawatsubashi S, Murata T, Lim J, et al. A histone chaperone, DEK, transcriptionally coactivates a nuclear receptor. Genes Dev. 2010;24:159–170.
16. Privette Vinnedge LM, Kappes F, Nassar N, Wells SI. Stacking the DEK: from chromatin topology to cancer stem cells. Cell Cycle. 2013;12:51–66.
17. Smith EA, Gole B, Willis NA, et al. DEK is required for homologous recombination repair of DNA breaks. Sci Rep. 2017;7:44662.
18. Kavanaugh GM, Wise-Draper TM, Morreale RJ, et al. The human DEK oncogene regulates DNA damage response signaling and repair. Nucleic Acids Res. 2011;39:7465–7476.
19. Deutzmann A, Ganz M, Schonenberger F, Vervoorts J, Kappes F, Ferrando-May E. The human oncoprotein and chromatin architectural factor DEK counteracts DNA replication stress. Oncogene. 2015;34:4270–4277.
20. Slovak ML, Gundacker H, Bloomfield CD, et al. A retrospective study of 69 patients with t(6;9)(p23;q34) AML emphasizes the need for a prospective, multicenter initiative for rare "poor prognosis" myeloid malignancies. Leukemia. 2006;20:1295–1297.
21. Logan GE, Mor-Vaknin N, Braunschweig T, et al. DEK oncogene expression during normal hematopoiesis and in Acute Myeloid Leukemia (AML). Blood Cells Mol Dis. 2015;54:123–131.
22. Koleva RI, Ficarro SB, Radomska HS, et al. C/EBPalpha and DEK coordinately regulate myeloid differentiation. Blood. 2012;119:4878–4888.
23. Wise-Draper TM, Mintz-Cole RA, Morris TA, et al. Overexpression of the cellular DEK protein promotes epithelial transformation in vitro and in vivo. Cancer Res. 2009;69:1792–1799.
24. Cheung TH, Quach NL, Charville GW, et al. Maintenance of muscle stem-cell quiescence by microRNA-489. Nature. 2012;482:524–528.
25. Carro MS, Spiga FM, Quarto M, et al. DEK Expression is controlled by E2F and deregulated in diverse tumor types. Cell Cycle. 2006;5:1202–1207.
26. Ageberg M, Gullberg U, Lindmark A. The involvement of cellular proliferation status in the expression of the human proto-oncogene DEK. Haematologica. 2006;91:268–269.
27. Mauch P, Constine L, Greenberger J, et al. Hematopoietic stem cell compartment: acute and late effects of radiation therapy and chemotherapy. Int J Radiat Oncol Biol Phys. 1995;31:1319–1339.
28. Dainiak N. Hematologic consequences of exposure to ionizing radiation. Exp Hematol. 2002;30:513–528.
29. Dent P, Yacoub A, Fisher PB, Hagan MP, Grant S. MAPK pathways in radiation responses. Oncogene. 2003;22:5885–5896.
30. Tesio M, Tang Y, Mudder K, et al. Hematopoietic stem cell quiescence and function are controlled by the CYLD-TRAF2-p38MAPK pathway. J Exp Med. 2015;212:525–538.
31. Hao S, Chen C, Cheng T. Cell cycle regulation of hematopoietic stem or progenitor cells. Int J Hematol. 2016;103:487–497.
32. Liu Y, Elf SE, Miyata Y, et al. p53 regulates hematopoietic stem cell quiescence. Cell Stem Cell. 2009;4:37–48.
33. Jayapal SR, Kaldis P. Cyclin E1 regulates hematopoietic stem cell quiescence. Cell Cycle. 2013;12:3588.
34. Karigane D, Kobayashi H, Morikawa T, et al. p38alpha activates purine metabolism to initiate hematopoietic stem/progenitor cell cycling in response to stress. Cell Stem Cell. 2016;19:192–204.
35. Wise-Draper TM, Morreale RJ, Morris TA, et al. DEK proto-oncogene expression interferes with the normal epithelial differentiation program. Am J Pathol. 2009;174:71–81.
36. Meyn MS, Lu-Kuo JM, Herzing LB. Expression cloning of multiple human cDNAs that complement the phenotypic defects of ataxia-telangiectasia group D fibroblasts. Am J Hum Genet. 1993;53:1206–1216.
37. Kappes F, Fahrer J, Khodadoust MS, et al. DEK is a poly(ADP-ribose) acceptor in apoptosis and mediates resistance to genotoxic stress. Mol Cell Biol. 2008;28:3245–3257.
38. Waldmann T, Baack M, Richter N, Gruss C. Structure-specific binding of the proto-oncogene protein DEK to DNA. Nucleic Acids Res. 2003;31:7003–7010.
39. Wang Y, Kellner J, Liu L, Zhou D. Inhibition of p38 mitogen-activated protein kinase promotes ex vivo hematopoietic stem cell expansion. Stem Cells Dev. 2011;20:1143–1152.
40. Wang Y, Liu L, Zhou D. Inhibition of p38 MAPK attenuates ionizing radiation-induced hematopoietic cell senescence and residual bone marrow injury. Radiat Res. 2011;176:743–752.
41. Waidmann S, Kusenda B, Mayerhofer J, Mechtler K, Jonak C. A DEK domain-containing protein modulates chromatin structure and function in Arabidopsis. Plant Cell. 2014;26:4328–4344.

Supplementary data

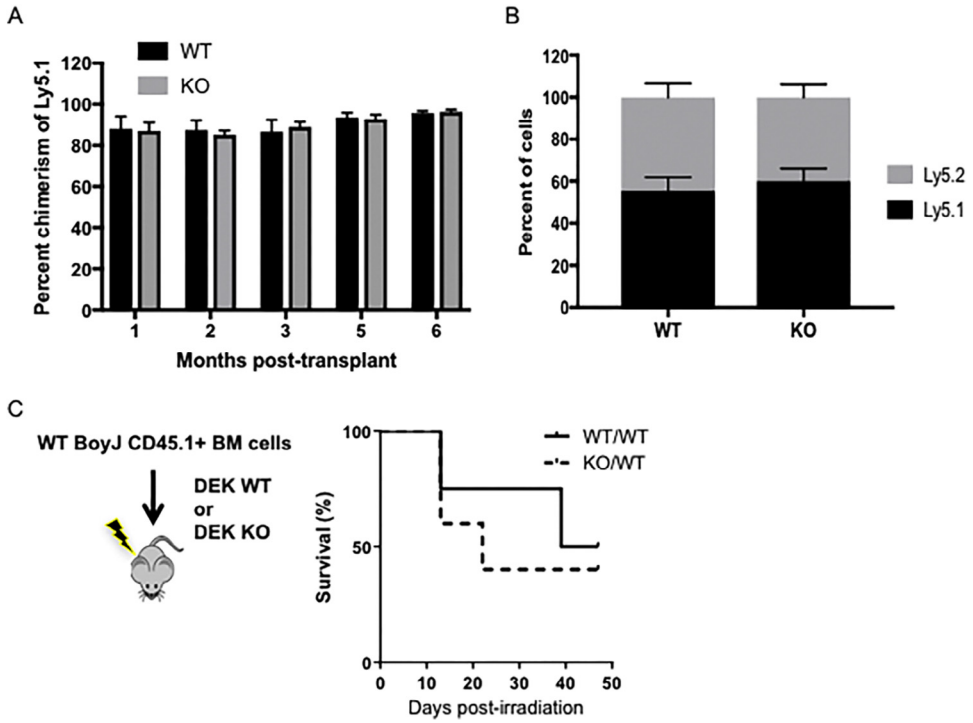

Supplementary Figure E1. There is no difference in bone marrow microenvironment or transplantation efficiency of HSCs from DEK WT and KO mice. (A) DEK WT (n = 5) and KO (n = 5) mice were lethally irradiated and transplanted with Ly5.1 bone marrow cells from BoyJ mice. Percent of BoyJ cells in the peripheral blood was measured for 6 months. (B) Competitive transplant assay, in which $1x10^6$ total bone marrow cells from DEK WT (n = 9) or KO (n = 9) mice were combined with $1x10^6$ total bone marrow cells from BoyJ mice and transplanted into lethally irradiated animals. Percentage of Ly5.1 (BoyJ) and Ly5.2 (C57Bl/6) cells were determined 3 weeks post-transplant. (C) Wild type CD5.1 + bone marrow cells from BoyJ mice were transplanted into irradiated DEK WT and KO animals. Animal survival following irradiation was recorded for 50 days.

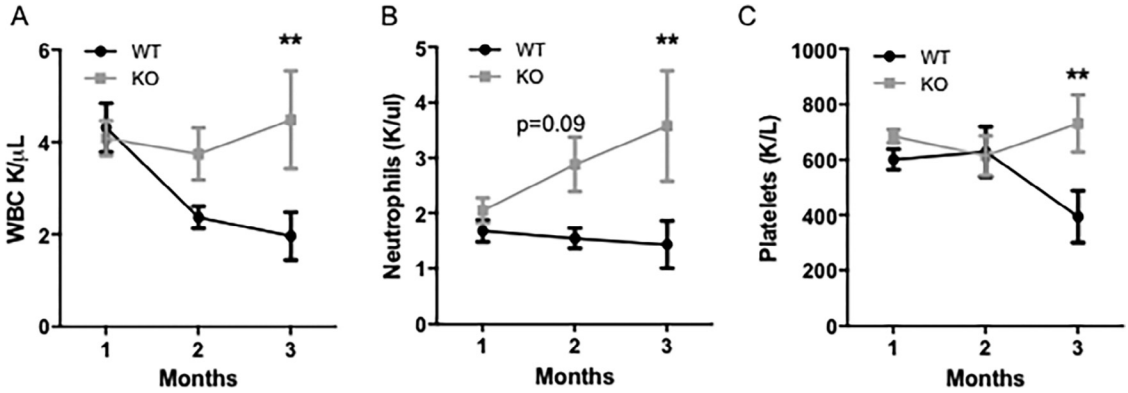

Supplementary Figure E2. Hematological response following repeated radiation exposure. (A) White blood cell, (B) neutrophil, and (C) platelet counts from the peripheral blood in DEK WT and KO mice over three months during repeated exposures to 7 Gy radiation (see Fig. 2A). DEK KO mice have maintained platelet counts and elevated neutrophil counts, which supports their prolonged survival.

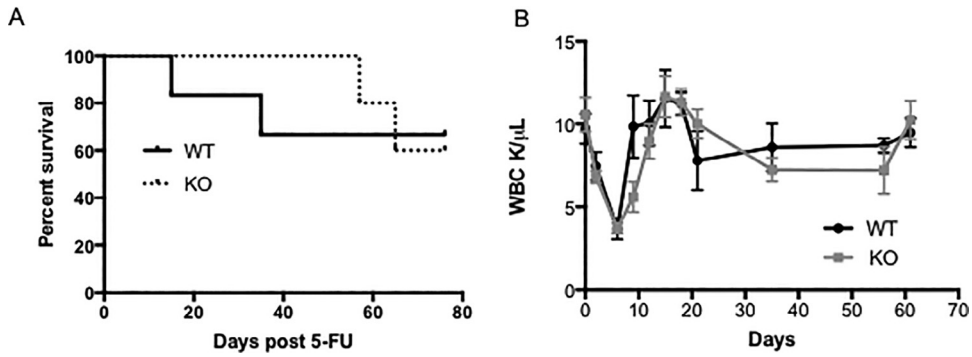

Supplementary Figure E3. Response to 5-fluorouracil treatment. (A) DEK WT (n = 6) and DEK KO (n = 5) mice were injected with 150 mg/kg 5-FU and animal survival was monitored for 76 days. (B) Total white blood cell (WBC) count of peripheral blood from 5-FU treated DEK WT and KO mice up to 61 days post treatment.

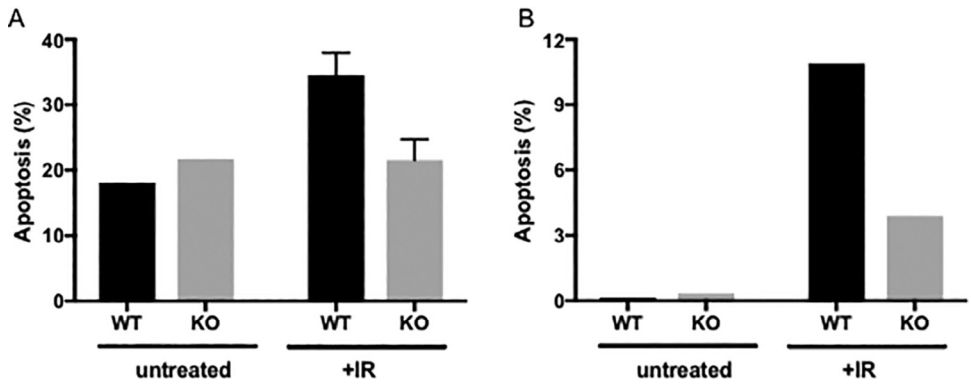

Supplementary Figure E4. DEK knockout cells have a decreased apoptosis response to radiation. (A) DEK WT (n = 1) and DEK KO (n = 2) mice were subjected to one dose of 7 Gy gamma radiation and monitored for apoptosis 24 hours later by sub-G1 analysis. (B) Mouse embryonic fibroblasts from DEK WT and KO cells [17, 18] were irradiated with a 30 Gy dose and analyzed for apoptosis 48 hours later by cleaved caspase 3 detection by flow cytometry.

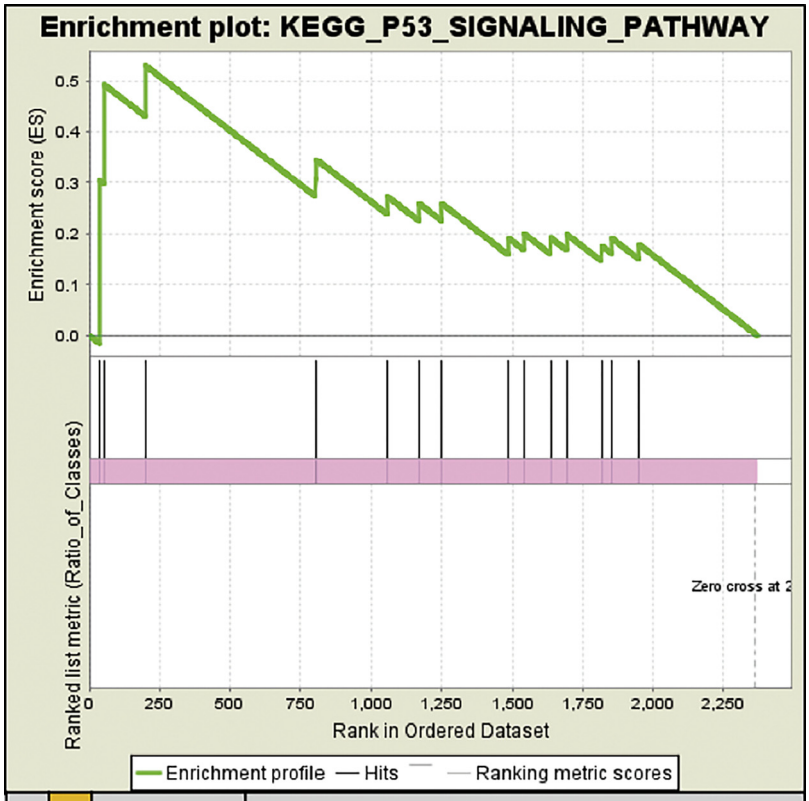

Dek KO	Dek WT	Gene Name	Description
		GADD45G	growth arrest and DNA-damage-inducible, gamma
		FAS	Fas (TNF receptor superfamily, member 6)
		IGF1	insulin-like growth factor 1 (somatomedin C)
		CCNB1	cyclin B1
		CDK4	cyclin-dependent kinase 4
		TSC2	tuberous sclerosis 2
		CDK2	cyclin-dependent kinase 2
		CCND2	cyclin D2
		GADD45B	growth arrest and DNA-damage-inducible, beta
		RRM2	ribonucleotide reductase M2 polypeptide
		GADD45A	growth arrest and DNA-damage-inducible, alpha
		CCND1	cyclin D1
		SESN3	sestrin 3
		BID	BH3 interacting domain death agonist
		RRM2B	ribonucleotide reductase M2 B (TP53 inducible)

Supplementary Figure E5. Differential expression of p53 pathway related genes in irradiated DEK KO and WT mice. Gene ontology analysis using GSEA of differentially regulated genes detected by RNA-Sequencing in irradiated DEK WT and KO MPP cells identified the p53 signaling pathway. Blue boxes depict the sample that had lower gene expression when comparing WT and KO MPP cells.